



OPEN

Indoxyl sulfate, a gut microbiome-derived uremic toxin, is associated with psychic anxiety and its functional magnetic resonance imaging-based neurologic signature

Christopher R. Brydges¹, Oliver Fiehn¹, Helen S. Mayberg^{2,3}, Henry Schreiber⁴, Siamak Mahmoudian Dehkordi⁵, Sudeepa Bhattacharyya⁶, Jungho Cha^{2,3}, Ki Sueng Choi^{2,3}, W. Edward Craighead^{7,8}, Ranga R. Krishnan⁹, A. John Rush^{5,10,11}, Boadie W. Dunlop^{3,15}✉, Rima Kaddurah-Daouk^{5,12,13,14}✉ & the Mood Disorders Precision Medicine Consortium*

It is unknown whether indoles, metabolites of tryptophan that are derived entirely from bacterial metabolism in the gut, are associated with symptoms of depression and anxiety. Serum samples (baseline, 12 weeks) were drawn from participants ($n = 196$) randomized to treatment with cognitive behavioral therapy (CBT), escitalopram, or duloxetine for major depressive disorder. Baseline indoxyl sulfate abundance was positively correlated with severity of psychic anxiety and total anxiety and with resting state functional connectivity to a network that processes aversive stimuli (which includes the subcallosal cingulate cortex (SCC-FC), bilateral anterior insula, right anterior midcingulate cortex, and the right premotor areas). The relation between indoxyl sulfate and psychic anxiety was mediated only through the metabolite's effect on the SCC-FC with the premotor area. Baseline indole abundances were unrelated to post-treatment outcome measures, and changes in symptoms were not correlated with changes in indole concentrations. These results suggest that CBT and antidepressant medications relieve anxiety via mechanisms unrelated to modulation of indoles derived from gut microbiota; it remains possible that treatment-related improvement stems from their impact on other aspects of the gut microbiome. A peripheral gut microbiome-derived metabolite was associated with altered neural processing and with psychiatric symptom (anxiety) in humans, which provides further evidence that gut microbiome disruption can contribute to neuropsychiatric disorders that may

¹West Coast Metabolomics Center, University of California, Davis, CA, USA. ²Department of Neurology and Neurosurgery, Icahn School of Medicine at Mount Sinai, New York, NY, USA. ³Department of Psychiatry and Behavioral Sciences, Emory University School of Medicine, Atlanta, GA, USA. ⁴Division of Biology & Biological Engineering, California Institute of Technology, Pasadena, CA, USA. ⁵Department of Psychiatry and Behavioral Sciences, Duke University School of Medicine, Durham, NC, USA. ⁶Department of Biological Sciences, Arkansas Biosciences Institute, Arkansas State University, Jonesboro, AR, USA. ⁷Department of Psychiatry and Behavioral Sciences, Emory University School of Medicine, Atlanta, GA 30329, USA. ⁸Department of Psychology, Emory University, Atlanta, GA, USA. ⁹Department of Psychiatry, Rush Medical College, Chicago, IL, USA. ¹⁰Department of Psychiatry, Health Sciences Center, Texas Tech University, Permian Basin, TX, USA. ¹¹Duke-National University of Singapore, Singapore, Singapore. ¹²Department of Medicine, Duke University, Durham, NC, USA. ¹³Duke Institute of Brain Sciences, Duke University, Durham, NC, USA. ¹⁴Duke University Medical Center, DUMC 3903, Blue Zone South, Durham, NC, USA. ¹⁵Emory University College of Medicine, 12 Executive Park Dr. NE, Room 347, Atlanta, GA 30329, USA. *A list of authors and their affiliations appears at the end of the paper. ✉email: bdunlop@emory.edu; kaddu001@mc.duke.edu

require different therapeutic approaches. Given the exploratory nature of this study, findings should be replicated in confirmatory studies.

Clinical trial NCT00360399 “Predictors of Antidepressant Treatment Response: The Emory CIDAR”
<https://clinicaltrials.gov/ct2/show/NCT00360399>.

The gut microbiota impacts numerous aspects of human health and disease¹, including neuropsychiatric disorders. The “microbiota–gut–brain axis” refers to a bidirectional communication pathway that connects the central nervous system (CNS), the gut, and the microbial community that inhabits the gastrointestinal tract². Within this axis, the gut microbiota modulates central processes through the activation of neuronal pathways (e.g., the vagus nerve) as well as through the production of microbial metabolites and immune mediators that can trigger changes in neurotransmission, neuroinflammation, and behavior^{3–6}.

Disruptions to the gut microbiome have been correlated with several neurological disorders, including Parkinson’s disease, autism spectrum disorder, schizophrenia, and major depressive disorder (MDD)^{7–10}, though the specific mechanisms that underlie the role of the gut microbiota in these diseases is not fully understood. However, research in preclinical rodent models shows that the gut microbiota is sufficient to alter host behavior, as shown by the increase in anxiety- and depressive-like behaviors in rodents after fecal microbiota transfer from humans with depression relative to those that received transfer of fecal microbiota from demographic controls^{11,12}. Further, transferred microbes resulted in altered metabolic states in the recipient mice that displayed depressive-like symptoms¹². These data implicate the gut microbiota as direct contributors to behaviors associated with depression and anxiety through their metabolic effects. In this study, we explore gut microbiota-associated tryptophan metabolism and correlate levels of metabolites to clinical symptoms and severity of depression and anxiety in humans.

Tryptophan is an essential amino acid that can be metabolized in the gastrointestinal tract via the serotonin, kynurenine, and indole metabolic pathways (Fig. 1), which have been associated with human maladies including autoimmunity, inflammatory diseases, metabolic syndrome, and neurological diseases including depression and anxiety disorders^{13,14}. Strikingly, the gut microbiota is exclusively responsible for the conversion of tryptophan to indole and indole derivatives, as there are no detectable levels of these molecules in gnotobiotic mice that lack a gut microbiome¹⁵. Analysis of biosynthetic pathways found that the genes necessary to make indole and indole derivatives, such as indole-3-propionic acid (IPA), indole-3-acetic acid (IAA), and indole-3-lactic acid (ILA), are found exclusively in the gut microbiome but not in mammalian genomes¹³ (Fig. 1). Indoxyl sulfate (IS), results from the sulfonation of bacterially-derived indole via sulfotransferases in human liver¹⁶; however, the rate of indoxyl sulfate production is driven by the presence of indole derivatives¹⁷, which are produced exclusively by gut microbes¹⁵. Importantly, these indoles can have immunomodulatory effects and are potent agonists for aryl hydrocarbon receptors¹⁸ (AHRs), which regulate host immunity and barrier function at mucosal sites¹⁹.

Indole derivatives can also affect immune status in the brain, as some indole derivatives (e.g., IPA and IAA) have anti-inflammatory effects on neurodegenerative diseases in the experimental autoimmune encephalomyelitis (EAE) mouse model of multiple sclerosis^{20,21} as well as in a cell line model of Alzheimer’s disease²². Several studies have examined the role of the brain gut axis, and indoles specifically, for their impact on physical health, cognition, and neurological disorders^{23–25}. High levels of the uremic toxin IS, which is normally cleared via the kidneys and excreted in the urine, is associated with diminished cognitive function in renal dialysis patients²⁶. IS is also associated with both neurodevelopmental and neurodegenerative diseases, as levels of IS are increased in patients who have an autism spectrum disorder²⁷ or Parkinson’s disease²⁸. Although the mechanistic role of IS in these diseases is unknown, IS can cross the blood–brain barrier²⁹ and can increase levels of oxidative stress and pro-inflammatory cytokine signaling in astrocytes and mixed glial cells *in vitro*³⁰, which suggests that inflammation and reactive oxygen species may be involved.

With respect to psychiatric disorders, IS has been associated with behavioral defects in preclinical models of anxiety and depression. The administration of IS into rodents’ drinking water results in increased concentrations of IS in the brain and increased blood–brain barrier permeability in an AHR-dependent manner, with accompanying increases in anxiety and cognitive deficits^{31,32}. Monocolonization experiments with indole-producing *Escherichia coli* and isogenic mutants have shown that indole production by gut bacteria is sufficient to drive increases in anxiety- and depressive-like behavior in rats³³. Although interest in the role of the brain gut axis for psychiatric disorders is growing, there are few human studies, with almost no work examining indoles specifically³⁴.

Taken together, the preclinical and clinical data indicate that indole derivatives provide excellent models to study the microbiota–gut–brain axis given their connection to central immune regulators (i.e., AHR), their link to human neurological diseases, and the exclusivity of indole production to gut microbes.

To date, the effects of peripheral metabolic concentrations on neural functioning have received little study, likely due to the paucity of datasets that contain concurrently collected metabolomic and neuroimaging measures. Such research is crucial for determining how changes in peripheral systems may yield alterations in brain function that can produce clinically relevant symptoms such as depression, anxiety, or cognitive impairment. Metabolomic data may prove to have clinical value by providing biological markers for identifying treatment-relevant subtypes of MDD, as an objective marker of change during treatment, and as a predictor of the longer-term course of illness. Beyond enhancing pathophysiological understanding (which could identify novel treatment targets), concurrently analyzing metabolomic and neuroimaging data may enable the development of easier-to-obtain peripheral blood markers that can act as surrogate markers for brain states relevant to disease pathology and personalization of treatments^{35,36}.

of any medically significant or unstable medication condition that could impact study participation, safety, or data interpretation, as assessed through a medical history, physical exam, electrocardiogram, and screening laboratory testing. Psychiatric exclusion criteria included a lifetime history of bipolar disorder, primary psychotic disorder, or dementia, or a diagnosis in the 12 months prior to baseline of obsessive–compulsive disorder, eating disorder, or dissociative disorder. Patients were also excluded if they met DSM-IV criteria for substance abuse within 3 months, substance dependence within 12 months of the randomization visit, or if their urine tested positive for drugs of abuse. Treatment was provided for 12 weeks with duloxetine (30–60 mg/day), escitalopram (10–20 mg/day), or CBT 16 individual 1-h sessions.

Symptom assessments. At the baseline visit, participants were assessed by trained interviewers using the HAM-D and the HAM-A. The HAM-A is a 14-item measure that consists of two subscales, “psychic anxiety” (items 1–6 and 14), and “somatic anxiety” (items 7–13)^{45,46}. Psychic anxiety consists of the symptoms of anxious mood, tension, fears, depressed mood, insomnia, impaired concentration, and restlessness. Somatic anxiety consists of physical symptoms associated with the muscular, sensory, cardiovascular, respiratory, gastrointestinal, genitourinary, and autonomic systems. Participants also completed the QIDS-SR, which assesses the nine diagnostic symptom criteria for MDD⁴⁷. The HAM-D, HAM-A, and QIDS-SR were repeated at the Week 12 visit.

Blood sampling. Participants who met all eligibility criteria at the baseline visit underwent an antecubital phlebotomy, without regard for time of day, diet, or fasting/fed status. Sampling was repeated at the week 12 visit. Collected samples were allowed to clot for 20 min and then centrifuged at 4 °C to separate the serum, which was frozen at – 80 °C until being thawed for the current analyses.

Neuroimaging. To explore associations between indole metabolites and brain function, we used the resting state fMRI (rs-fMRI) scans collected during the week prior to baseline, the details of which have previously been published⁴³. Briefly, eyes-open scanning was performed for 7.4 min in a 3-T Siemens TIM Trio (Siemens Medical Systems, Erlangen, Germany). Image analysis was conducted using AFNI^{48,49}. [Analysis of Functional NeuroImages] software package. The standard preprocessing pipeline implemented in AFNI package was used for processing rs-fMRI data. The time series of rs-fMRI data were despiked, and then corrected for motion and slice-time acquisition. Scans with head motion > 2 mm in any direction were excluded from the analysis. The remaining effects of the noise signal, including residual head motion inferences, signal from the CSF and local white matter, were also corrected. Subsequently, data were applied a band-pass filter and smoothed using an isotropic Gaussian kernel of 8 mm full width at half maximum. The imaging anatomical and functional data sets were co-registered and normalized to standard Montreal Neurological Institute (MNI) 1-mm voxel space. Consistent with our prior analyses⁴², we used a region-of-interest seed-based approach to assess the resting state functional connectivity (RSFC) of the SCC. The SCC volume was defined using the Harvard–Oxford Atlas⁵⁰, and the SCC was thresholded at 50% probability centered on MNI coordinates 66, 24, –11. The seeds comprised two 5-mm radius spheres, with a final volume of 485 mL each. Utilizing 3dNetCorr⁵¹, the mean time course of the bilateral seed was correlated voxel-wise with the rest of the brain. The voxelwise correlation coefficients were then z-scored by calculating the inverse hyperbolic tangent, yielding the seed-based RSFC maps for analysis.

Metabolomics data acquisition. Metabolomics data focused on primary and polar metabolites using gas chromatography—time of flight mass spectrometry⁵². Briefly, 30 µL of plasma was extracted at – 20 °C with 1 mL degassed isopropanol/acetonitrile/water (3/3/2). Extracts were dried down, cleaned from triacylglycerides using acetonitrile/water (1/1), and derivatized with methoxyamine and trimethylsilylation. Samples (0.5 µL) were injected at 250 °C to a 30 m rtx5-SiLMS column, ramped from 50 to 300 °C at 15 °C/min, and analyzed by – 70 eV electron ionization at 17 spectra/s. Raw data were deconvoluted and processed using ChromaTOF vs. 4.1 and uploaded to the UC Davis BinBase database⁵³ for data curation and compound identification⁵⁴. Result data were normalized by SERRF software to correct for drift or batch effects⁵⁵.

Statistical analyses. Indole abundance and ratios of each indole pair were included in all analyses. In order to investigate the role of indoles in depression and anxiety symptomology at baseline, partial Spearman rank correlations were conducted between the baseline abundance/ratio of each indole and HAM-D 17-item total score, HAM-A total score, HAM-A Psychic and Somatic subscores, QIDS-SR 16-item total score, and each individual QIDS-SR item after accounting for age, sex, and body mass index (BMI). Spearman correlations were also conducted between baseline indole abundance/ratio and participant demographic factors (age, BMI, height, and weight). Additionally, sex differences in baseline indole abundance/ratio were tested using Mann–Whitney *U* tests and fold changes in median abundance/ratio between groups.

To investigate the potential effects of treatment on indoles, changes in indole abundance from pre- to post-treatment were tested using Wilcoxon signed-rank tests and fold changes. Partial Spearman rank correlations were conducted between post-treatment indole abundance/ratio and post-treatment HAM-D 17-item total score, HAM-A total score, and HAM-A Psychic and Somatic subscores, QIDS-SR 16-item total score, and each individual QIDS-SR item, after accounting for age, sex, and baseline BMI. The same analyses were also conducted with change from pre- to post-treatment scores of all psychiatric variables, and also with fold changes from pre- to post-treatment for each indole. We also evaluated categorical outcomes at week 12 for four outcome groups, as defined previously^{43,56}: “Remitter” (HAM-D ≤ 7); “Response without remission” (≥ 50% reduction from baseline HAM-D, but not reaching remission threshold); “Partial response” (30–49% reduction from baseline HAM-D); and “Treatment failure” (< 30% reduction from baseline HAM-D score).

Variable	N (%) (N = 196)
Sex (Female)	122 (62.2%)
Race	
White	73 (37.2%)
Native American	58 (29.6%)
Black	38 (19.4%)
Asian	2 (1.0%)
Multiracial	14 (7.1%)
Unknown/not reported	11 (5.6%)
Hispanic ethnicity (%)	77 (39.3%)
Mean (SD)	
Age (years)	39.11 (11.77)
Body mass index	28.73 (6.27)
HAM-D 17-item total score (baseline)	19.76 (3.77)
QIDS-SR total score (baseline)	14.27 (3.83)
HAM-A total score (baseline)	16.28 (5.37)
HAM-A psychic anxiety subscale score (baseline)	10.79 (2.69)
HAM-A somatic anxiety subscale score (baseline)	5.48 (3.73)
HAM-D 17-item total score (post-treatment)	7.19 (6.11)
QIDS-SR total score (post-treatment)	5.05 (4.25)
HAM-A total score (post-treatment)	6.64 (5.82)
HAM-A psychic anxiety subscale score (post-treatment)	4.08 (3.62)
HAM-A somatic anxiety subscale score (post-treatment)	2.56 (3.12)

Table 1. Subject demographic and clinical characteristics. *HAM-A* Hamilton Anxiety Rating Scale, *HAM-D* Hamilton Depression Rating Scale, *QIDS-SR* Quick Inventory of Depressive Symptomatology, Self-report.

Differences in indole post-treatment abundance/ratio and fold change were investigated between each pair of treatment response outcome groups³² (treatment failure; partial response; response; remission) by conducting Mann–Whitney *U* tests. This analysis was also repeated with baseline indole abundances/ratios to investigate whether baseline levels of indoles may be associated with treatment outcome. Although statistical power was reduced by splitting the sample, we also explored whether there were differential changes in indoles between patients treated with CBT versus antidepressant medication and their within-treatment outcomes. All reported *p*-values were adjusted for multiple comparisons using the Holm method within each psychometric measure (i.e., Holm correction was applied to each statistical test within each measure). This correction was applied in order to decrease the Type I error rate, whilst also maintaining a low enough Type II error rate given the exploratory nature of the hypotheses⁵⁷.

Neuroimaging analyses were conducted using AFNI³⁶ and jamovi (www.jamovi.org). Of 122 participants who had an adequate quality of resting-state fMRI data⁴³, 80 had metabolomic measurements and clinical scores. Voxel-wise linear regression analyses were performed to examine the relationship between SCC-FC and IS or psychic anxiety scores (uncorrected $p < 0.005$ and > 250 voxels cluster size). A conjunction analysis identified overlapping areas between the SCC-FC of IS and the SCC-FC of psychic anxiety scores. Subsequently, mediation analyses were performed using the Medmod module⁵⁸ in jamovi. Three regions identified by the whole brain linear regression analysis between SCC-FC and IS were used for the mediation analysis. We explored each region, and combinations of the three regions, in the mediation models. For each model, the direct and indirect effects were estimated using bootstrapping with 5000 samples.

Results

Of the 344 patients randomized in PRiEDICT, 196 had metabolomic measures available for analysis at baseline and 124 were available at week 12 ($n = 34$ CBT; $n = 44$ duloxetine; $n = 46$ escitalopram). The demographic and clinical characteristics of the 196 participants are presented in Table 1.

Baseline associations. *Associations of indole metabolites with demographic variables.* Supplemental Fig. 1 shows a heat map of correlations between baseline indole abundance/ratio and participant demographic variables. Abundance of ILA was positively associated with age, height, and weight (all $r_s > 0.18$, all $p_s < 0.040$). The ratios of IAA/ILA (negative associations) and ILA/IS (positive associations) were also significantly associated with height and weight (all $p_s < 0.034$). For sex differences, abundance of IAA (Fold Changes (FC) = 1.19, $p = 0.039$) and ILA (FC = 1.37, $p < 10^{-9}$), and ratios of ILA/IPA (FC = 1.40, $p = 0.004$) and ILA/IS (FC = 1.16, $p = 0.013$) were all found to be significantly higher in men than in women.

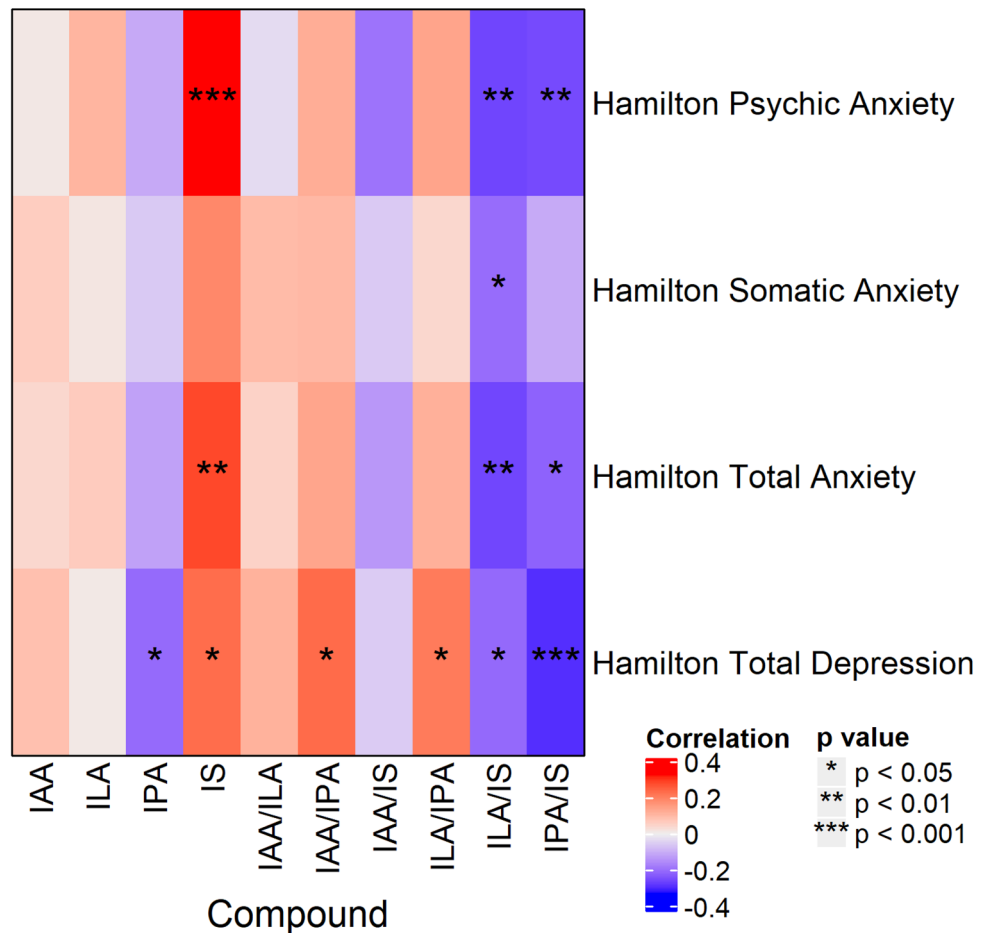


Figure 2. Heat map of Holm-corrected partial Spearman rank correlations between baseline indole abundance/ratio and Hamilton Anxiety scores and Hamilton Depression scores, after accounting for age, sex, and BMI.

Associations of indole metabolites with depression and anxiety. Figure 2 shows a heat map of correlations between baseline indole abundance/ratio and baseline levels of the HAM-D total score, Hamilton Anxiety Rating Scale (HAM-A)⁴⁶ total score, and HAM-A psychic and somatic subscores. Greater abundance of IS was associated with higher scores on the HAM-D 17-item total score ($r=0.21$, $p=0.018$), HAM-A total score ($r=0.26$, $p=0.002$), and HAM-A psychic subscore ($r=0.31$, $p=0.0001$), but not on the HAM-A somatic subscore. Additionally, the ratios of ILA/IS and IPA/IS were negatively correlated with HAM-A total and psychic scores (all $r_s > -0.20$, all $p_s < 0.033$), for which a negative correlation indicates that increasingly severe symptoms are associated with a relative increase in IS and/or a relative decrease in ILA or IPA. Additionally, IPA/IS was negatively correlated with HAM-D total score ($r=-0.24$, $p=0.001$).

The same analyses were conducted with the sample stratified by sex (see Supplemental Figs. 2 and 3). The pattern of correlations between groups was similar, although there were more significant correlations in the female sample, likely due to greater statistical power. In particular, IS was positively correlated with HAM-A psychic subscore in the females ($r=0.32$, $p=0.002$) and the males, but the correlation in the male group did not reach statistical significance ($r=0.28$, $p=0.071$).

Associations of indole metabolites with individual symptoms of depression. Correlations between Quick Inventory of Depressive Symptoms-Self-Report (QIDS-SR)⁴⁷ items, and total scores and indole abundances/ratios are presented in Fig. 3. Of note, IS positively correlated with items 4 (hypersomnia; $r=0.22$, $p=0.016$) and 6 (decreased appetite; $r=0.20$, $p=0.034$), and the IPA/IS ratio negatively correlated with QIDS-SR total score ($r=-0.21$, $p=0.027$). The same analyses were conducted with the sample stratified by sex (see Supplemental Figs. 4 and 5). In the females, IAA/IS and IPA/IS negatively correlated with item 5 (feeling sad; $r_s = -0.28$ and -0.25 , $p_s = 0.009$ and 0.030 , respectively) and QIDS-SR total score ($r_s = -0.23$ and -0.25 , $p_s = 0.049$ and 0.029 , respectively). In the males, item 13 (general interest) was positively correlated with IS ($r=0.33$, $p=0.021$), and item 15 (feeling slowed down) was positively correlated with IAA ($r=0.33$, $p=0.026$).

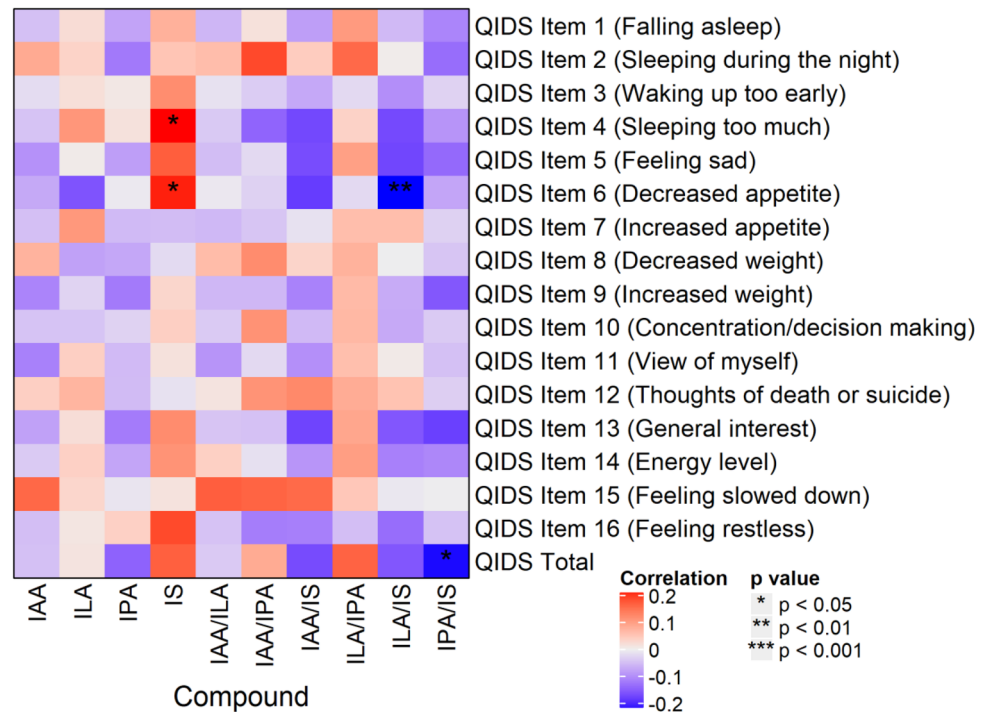


Figure 3. Heat map of Holm-corrected partial Spearman rank correlations between baseline indole abundance/ratio and QIDS-SR items and total score, after accounting for age, sex, and BMI. QIDS-SR 16-item Quick Inventory of Depressive Symptomatology-Self-Rated.

Treatment effects. Compound abundance significantly increased from pre- to post-treatment for ILA (FC = 1.05, $p = 0.006$), but not for any other compound/ratio (all $ps > 0.12$). This indicates that the treatments had limited overall effect on indole composition and levels.

For post-treatment indole abundances and ratios, there were significant correlations between IAA/IS and QIDS-SR item 15 (feeling slowed down; $r = 0.30$, $p = 0.007$). Additionally, post-treatment ILA abundance was significantly higher in men than in women (FC = 1.24, $p = 0.00001$), as was the ILA/IPA ratio (FC = 1.54, $p = 0.002$). Conversely, the IPA/IS ratio was lower in men than in women (FC = 0.80, $p = 0.048$). No other significant post-treatment effects were observed.

For fold changes, change in IAA/IS ratio correlated with post-treatment scores of QIDS-SR item 5 (feeling sad; $r = 0.27$, $p = 0.032$). No significant associations were observed when correlating indole fold changes with any other post-treatment scores, or with change in depression/anxiety scores (all $ps > 0.10$). Additionally, no sex differences were observed for fold changes (all $ps > 0.07$), and no differences in fold changes were observed between response outcome groups (all $ps > 0.12$).

Baseline levels of indoles and their ratios did not significantly correlate with changes in symptoms for any measure or item (all $rs < 0.15$, $ps > 0.59$). Comparison of categorical response outcomes also showed no meaningful differences in baseline indole abundances or ratios. These analyses indicate that pre-treatment indole compound abundances are not predictive of eventual treatment outcomes.

Treatment-specific effects. Exposure to CBT or medication (i.e., regardless of outcome) was associated with differential changes in indole measures. Medication-treated patients demonstrated increases in IPA (FC = 1.28, $p = 0.005$) and ILA (FC = 1.09, $p = 0.007$) and decreases in the IAA/IS ratio (FC = 0.95, $p = 0.035$) and IAA/IPA ratio (FC = 0.91, $p = 0.002$). In contrast, CBT-treated patients had an increase in the IAA/IPA ratio (FC = 1.56, $p = 0.030$).

No baseline indole measures emerged as statistically significant moderators to predict differential outcomes for the two treatments. There were also no statistically significant differences between treatments in terms of the strength of the correlations between changes in rating scale scores and individual symptom items with changes in indole measures (all $p > 0.19$). However, examining the within-treatment categorical outcomes found that remitters to medication had a significant increase in IPA (FC = 1.32, $p = 0.005$) and decrease in ILA/IPA (FC = 0.78, $p = 0.049$), whereas remitters to CBT had a significant decrease in IPA/IS (FC = 0.54, $p = 0.049$).

Associations of indoxyl sulfate with brain resting state functional connectivity. Given the observed association between IS and psychic anxiety, relationships of Subcallosal Cingulate Cortex-Functional Connectivity (SCC-FC) with IS and with psychic anxiety scores were investigated (see Fig. 4). IS abundance was positively correlated with SCC-FC with the bilateral anterior insula, anterior midcingulate cortex (aMCC), sup-

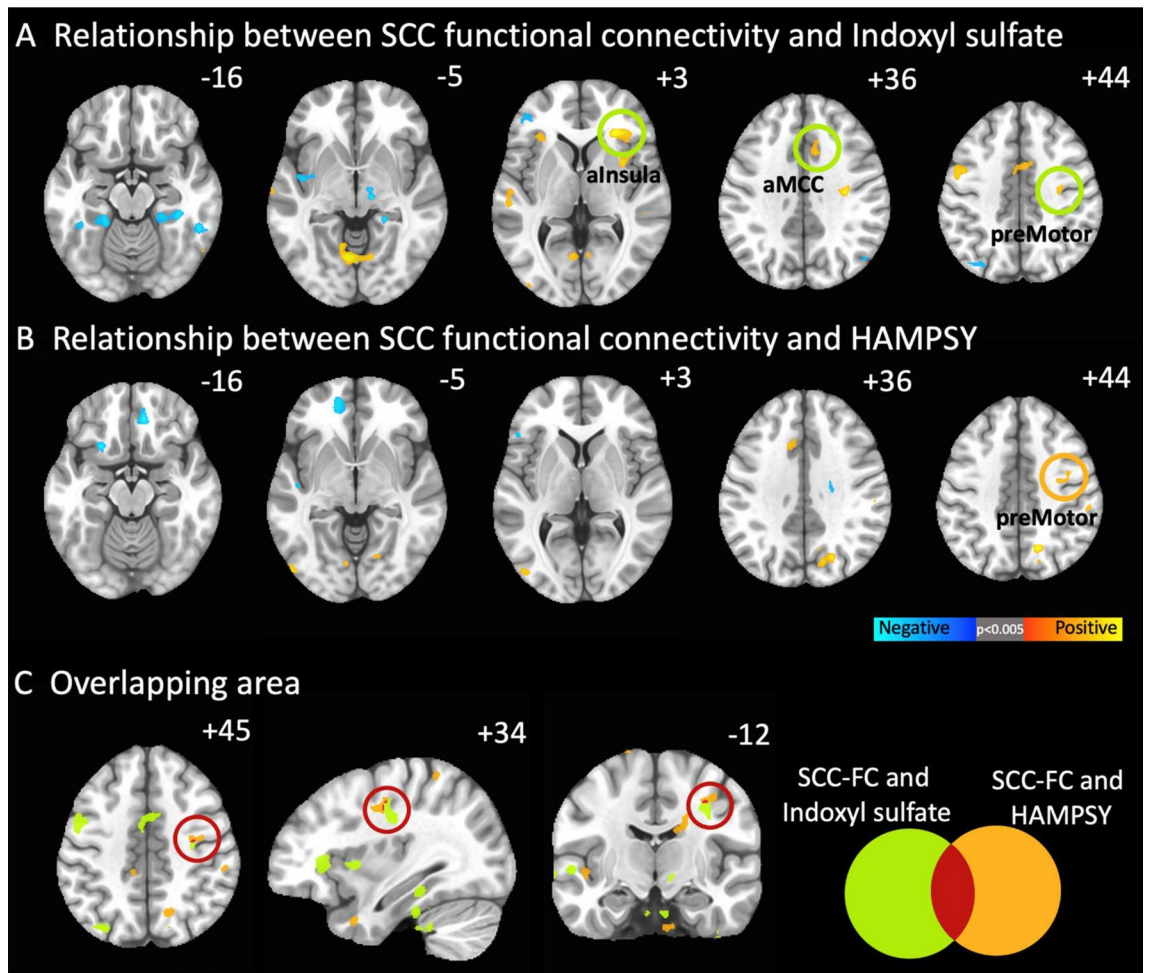


Figure 4. Resting state functional connectivity of subcallosal cingulate cortex (SCC) associations with peripheral indoxyl sulfate abundances and psychic anxiety scores. **(A)** SCC functionally connected regions showing a significant correlation with indoxyl sulfate abundances. Orange circles identify regions incorporated into the mediation models. **(B)** SCC functionally connected regions showing a significant correlation with psychic anxiety scores. Green circle identifies right premotor region. **(C)** Conjunction analysis: SCC functionally connected region showing a significant correlation with both indoxyl sulfate abundances and psychic anxiety scores. The red circle indicates the only region to emerge in this analysis, the right premotor region. *HAMPSY* Psychic anxiety subscore of the Hamilton Anxiety Rating Scale. *SCC-FC* subcallosal cingulate cortex functional connectivity.

plementary motor area (SMA), and right premotor area (Fig. 4A). Psychic anxiety scores showed a significant positive correlation with SCC-FC with the left aMCC, right precuneus, and right premotor area; there was a negative correlation with SCC-FC with the ventromedial prefrontal cortex, right orbitofrontal, and left Brodmann Area 47 (Fig. 4B). The conjunction analysis identified one overlapping area: the right premotor region (Fig. 4C).

The mediation analyses explored whether the association of IS with psychic anxiety was mediated through its effects on SCC-FC. Figure 5A shows the overall association between IS and psychic anxiety ($z = 1.976$, $p = 0.048$). Figure 5B shows that the identified overlapping area in the SCC-FC analyses—the right premotor region—mediated the association between IS and psychic anxiety (indirect pathway: $z = 2.138$, $p = 0.033$). Because our whole brain SCC-FC analyses had also found IS concentrations to be significantly associated with two other regions previously identified in neuroimaging studies of anxiety (the right anterior insula and the aMCC, Fig. 4A), we conducted further mediation analyses incorporating these two regions along with the right premotor region. Even though the three regions were highly correlated with each other in their functional connectivity to SCC (Fig. 5C), only the right premotor region mediated the relationship between IS and psychic anxiety scores when all three regions were included in the model (Fig. 5D, indirect pathway: $z = 1.991$, $p = 0.046$).

Discussion

Increasing evidence suggests that gut bacteria can complement human metabolism, and that together they define the metabolome comprised of the collection of small molecules in blood and in different organs. Bacteria can further metabolize compounds available through human metabolism, food-intake, and/or human ingestion of chemicals. Also, humans can further metabolize compounds produced by bacteria, which results

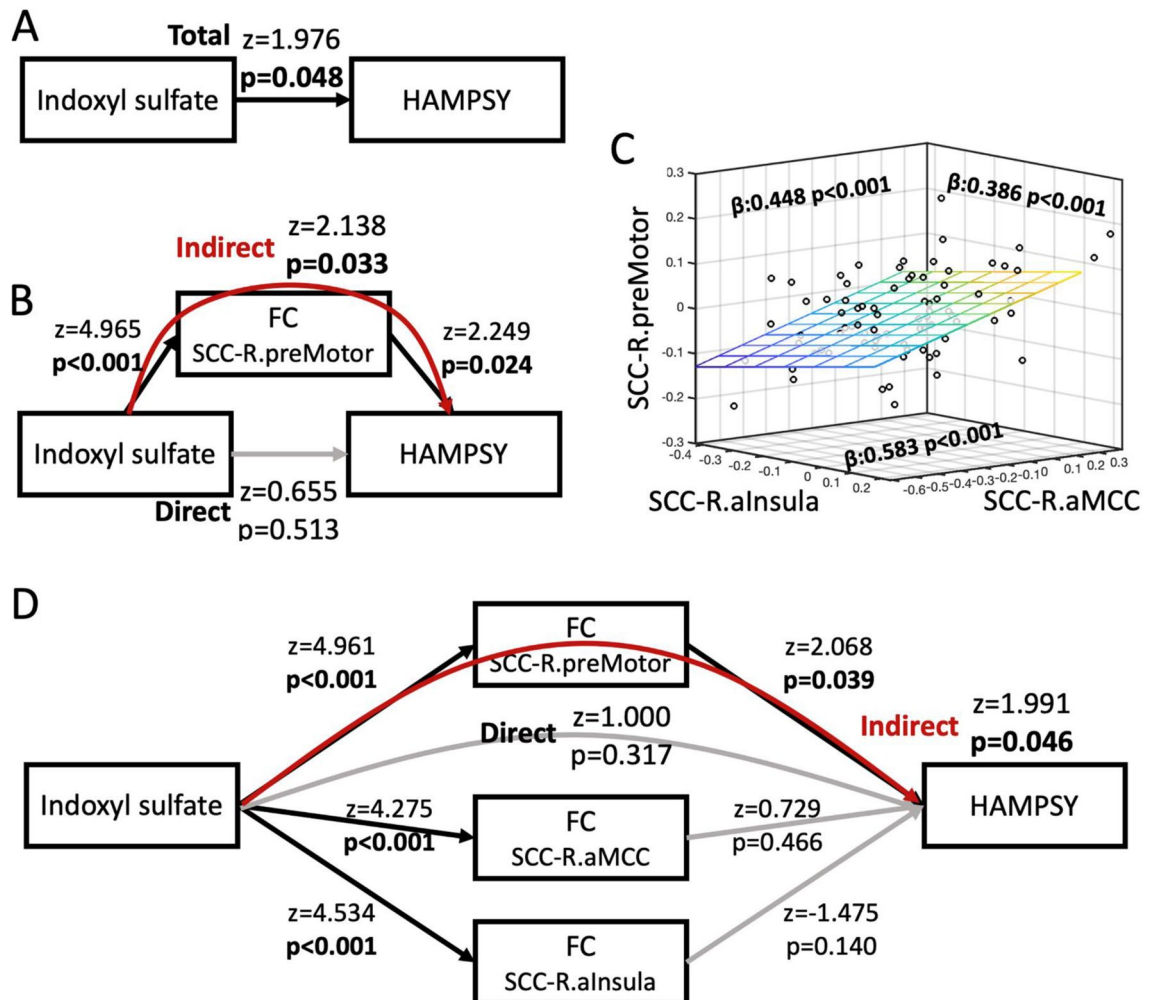


Figure 5. The impact of indoxyl sulfate on psychic anxiety scores is mediated by its effects on the resting state functional connectivity between the subcallosal cingulate cortex and the right premotor region. **(A)** Association between indoxyl sulfate and psychic anxiety scores. **(B)** Mediation model incorporating the overlapping area, right premotor region, indicating that the effect of indoxyl sulfate on psychic anxiety is mediated via its effects on the functional connectivity between the SCC and right premotor region. **(C)** Significant SCC-FC correlations between the right anterior insula, right anterior midcingulate cortex, and right premotor region, which were included in the mediation model shown in **(D)**. **(D)** Full mediation model incorporating the three regions showing significant SCC-FC correlations with indoxyl sulfate abundances. Although indoxyl sulfate is significantly correlated with all three regions, only the pathway through the right premotor region significantly mediates indoxyl sulfate's effect on psychic anxiety. Black lines indicate significant associations within the model; grey lines are insignificant associations. Red line indicates significant mediation of indoxyl sulfate on psychic anxiety through the indirect pathway of right premotor SCC-FC. *HAMPSY* Psychic anxiety subscore of the Hamilton Anxiety Rating Scale. *SCC-FC* subcallosal cingulate cortex functional connectivity.

in human-bacteria co-metabolism and the production of a large number of chemicals that can impact human health, including brain function. Examples include the metabolism of cholesterol and its clearance mediated by bacteria, which can produce secondary bile acids that we recently implicated in the pathogenesis of Alzheimer's disease^{59,60}. Several compounds produced from the metabolism of phospholipids and choline by gut bacteria lead to compounds like trimethylamine N-oxide, which have been implicated in cardiovascular diabetes and CNS disease^{61,62}.

Indoles represent a class of gut bacterially-derived compounds that are produced from tryptophan, an essential amino acid that can also be converted (through separate pathways) into tryptamine, serotonin, skatol, and melatonin, among other metabolites involved in CNS functioning and diseases. Mounting evidence suggests that indoles derived from gut bacterial metabolism exert significant biological effects and may contribute to the etiology of cardiovascular, metabolic, and psychiatric diseases. To date, research in this area has been mainly limited to experimental studies in model systems.

In this investigation, we interrogated levels of four indoles produced by gut bacteria and their relationship to anxiety and depression severity and response to treatment. At baseline, IS abundance was found to positively correlate with severity of Psychic Anxiety and total anxiety. IPA seems protective, as noted earlier, indicating

that indoles, as a class, can have mixed effects on neuropsychiatric health. Different strains of bacteria can lead to the production of different indoles; for example, tryptophanase-producing bacteria produce toxic IS while *Clostridium sporogenes* and other bacterial strains produce protective IPA^{63,64}. Notably, IS levels did not meaningfully change with treatment, and changes in IS were not correlated with improvement in depression or anxiety measures. This suggests that for patients who do not benefit from standard treatments, a novel therapeutic approach may be to modulate gut microbiome composition and activity.

This association between IS and anxiety may reflect an impact of IS on the functional connectivity between the SCC and the right premotor region. IS abundances were also associated with greater connectivity of the SCC with a well-established network for the processing and control of emotionally salient, particularly aversive, stimuli, comprising the anterior insula and aMCC. The anterior insula, aMCC, and supplementary motor area form a network that is involved in the attention to, interpretation of, and control of emotional responses^{65–69}, and greater activity in this network correlates positively with subjective anxiety^{70,71}. The premotor cortex is functionally and structurally connected to the SMA and the aMCC, which act together in the preparation and readiness for voluntary movement in response to internal and external stimuli⁷². The aMCC also functions as a site of integration for the processing of pain and motor control⁷³. Outputs from this network include projections to the spinal cord and adrenal medulla⁷⁴, which may contribute to the sympathetic arousal and heightened cortisol release under situations of psychic stress. Taken together, an interpretation of these results is that the co-metabolism of tryptophan by certain gut microbiota that result in the production of IS may induce anxiety through the activation of established brain networks, and that existing treatments do not specifically resolve this pathogenetic process when they lead to clinical improvement.

Although the activity of the premotor cortex has not been a major focus in studies of anxiety and depression, Pierson and colleagues⁷⁵, using the electroencephalography measure of contingent negative variation (which localizes to the premotor cortex⁷⁶), demonstrated abnormal activation of this region in anxious MDD patients compared to MDD patients with psychomotor retardation. Ma and colleagues⁷⁷ found that patients with generalized anxiety disorder have increased resting state functional connectivity between the habenula and right premotor cortex. Others have found abnormal premotor function or connectivity in social anxiety disorder^{71,78}. Studies of healthy controls revealed that premotor cortex is significantly involved in processing abstract emotional concepts⁷⁹ and in threat anticipation, perhaps reflecting an unconscious preparation for action⁸⁰.

Our finding of a positive association between IS and connectivity of the SCC and the insula bilaterally is consistent with the insula's known involvement in processes relevant to anxiety, including emotional salience⁸¹, empathy for others' pain, and processing of uncertainty^{67,82–84}. In contrast, we did not find an association between IS abundances and somatic anxiety scores, nor was there an association of IS abundances with functional connectivity of the SCC-posterior insula, the insular region involved in sensorimotor integration. This reveals the specificity of the IS-anterior insula association for psychic anxiety.

The preceding discussion of the significant associations between the peripheral indole concentrations and brain network activity assumes that the direction of effect is that the metabolites are impacting brain function. However, because the gut-brain axis is bidirectional we cannot rule out the possibility that the brain activity patterns observed could have been contributing to the environment and activity of the gut to result in the observed metabolomic profiles.

Conceptualizing psychic anxiety as a chronic aversive stimulus akin to long-term pain may explain the positive correlation between higher IS levels and the QIDS-SR loss of appetite item. In mice, inflammatory pain is inhibited in the presence of hunger, mediated by neuropeptide Y signaling in the parabrachial nucleus⁸⁵. The association of higher IS concentrations with both reduction in appetite and increased connectivity between brain regions involved in pain processing (anterior insula and aMCC) may indicate that the symptom of low appetite reflects a compensatory response to this chronic anxiety-type pain. The observed positive correlations between change in change in the IAA/IS ratio items 15 (“Feeling slowed down”) and 5 (“Feeling sad”) also warrant comment. First, these results indicate that changes in the relative concentrations across the individual indole metabolites may have greater explanatory value than considering the individual metabolites in isolation. Second, the positive association of the IAA/IS ratio with item 15 is consistent with our conclusion that IS is particularly relevant for anxiety states, given that psychomotor slowing is rare in anxious depressed outpatients.

Limitations of this study include the absence of a healthy control comparison group and the inability to control for diet and fasting status. We did not pre-specify the items on the QIDS-SR to evaluate, so the identified associations should be considered tentative until replicated. We lacked fecal samples to analyze which would have allowed for a more direct correlation between specific gut microbiome species and the IS measures. We could not determine whether IS is the etiological agent of the anxiety because IS also acts to reduce the integrity of the blood brain barrier³², thereby creating the possibility that CNS penetration by an alternative molecule in the periphery is responsible for the observed association between anxiety and IS.

Taken together, our results indicate that increases in IS are associated with greater connectivity within an established brain network that is involved in the processing and control of aversive stimuli, but that the conscious experience of anxiety depends upon the degree of IS-related activation of SCC-right premotor cortex functional connectivity. The absence of an association between psychic anxiety scores and anterior insula/aMCC SCC-FC (Fig. 4B) may indicate that although IS concentrations are associated with level of connectivity of this control network in all patients, it is only when network function is inadequate that psychic anxiety ensues in conjunction with premotor activation in preparation for action⁸⁶. These analyses reveal the potential of integrated peripheral metabolomic-neuroimaging analyses to reveal mechanistic pathways that are associated with neuropsychiatric symptoms, especially for characterizing the pathological impact of specific gut microbiome-derived metabolites.

Although our results require replication before they can be applied in clinical practice, this work emphasizes several important considerations for investigations into the impact of metabolomics on psychiatric disorders. Among these considerations are the need to take into account the clinical heterogeneity of the DSM-defined

disorders when examining effects of metabolites, the importance of evaluating all components within a metabolic pathway rather than single metabolites, and the tremendous potential of integrating neuroimaging and metabolomics analyses for understanding pathophysiology and developing surrogate markers of brain function relevant to the diagnosis and treatment of psychiatric disorders.

Received: 6 May 2021; Accepted: 15 September 2021

Published online: 25 October 2021

References

- Frank, D. N. & Pace, N. R. Gastrointestinal microbiology enters the metagenomics era. *Curr. Opin. Gastroenterol.* **24**, 4–10 (2008).
- Foster, J. A. & Neufeld, K. A. M. Gut–brain axis: How the microbiome influences anxiety and depression. *Trends Neurosci.* **36**, 312–315 (2013).
- Sherwin, E., Sandhu, K. V., Dinan, T. G. & Cryan, J. F. May the force be with you: The light and dark sides of the microbiota–gut–brain axis in neuropsychiatry. *CNS Drugs* **30**, 1019–1041 (2016).
- Kelly, J. R. *et al.* Breaking down the barriers: The gut microbiome, intestinal permeability and stress-related psychiatric disorders. *Front. Cell. Neurosci.* **9**, 392 (2015).
- Sampson, T. R. & Mazmanian, S. K. Control of brain development, function, and behavior by the microbiome. *Cell Host Microbe* **17**, 565–576 (2015).
- Forsythe, P. & Kunze, W. A. Voices from within: Gut microbes and the CNS. *Cell Mol. Life Sci.* **70**, 55–69 (2013).
- Adams, J. B., Johansen, L. J., Powell, L. D., Quig, D. & Rubin, R. A. Gastrointestinal flora and gastrointestinal status in children with autism—comparisons to typical children and correlation with autism severity. *BMC Gastroenterol.* **11**, 22 (2011).
- Li, C. *et al.* Gut microbiota differs between Parkinson's disease patients and healthy controls in northeast China. *Front. Mol. Neurosci.* **12**, 171 (2019).
- Aizawa, E. *et al.* Possible association of Bifidobacterium and Lactobacillus in the gut microbiota of patients with major depressive disorder. *J. Affect Disord.* **202**, 254–257 (2016).
- Xu, R. *et al.* Altered gut microbiota and mucosal immunity in patients with schizophrenia. *Brain Behav. Immun.* **85**, 120–127 (2020).
- Kelly, J. R. *et al.* Transferring the blues: Depression-associated gut microbiota induces neurobehavioural changes in the rat. *J. Psychiatr. Res.* **82**, 109–118 (2016).
- Zheng, P. *et al.* Gut microbiome remodeling induces depressive-like behaviors through a pathway mediated by the host's metabolism. *Mol. Psychiatry* **21**, 786–796 (2016).
- Agus, A., Planchais, J. & Sokol, H. Gut microbiota regulation of tryptophan metabolism in health and disease. *Cell Host Microbe* **23**, 716–724 (2018).
- Gao, J. *et al.* Impact of the gut microbiota on intestinal immunity mediated by tryptophan metabolism. *Front. Cell Infect. Microbiol.* **8**, 13 (2018).
- Wikoff, W. R. *et al.* Metabolomics analysis reveals large effects of gut microflora on mammalian blood metabolites. *Proc. Natl. Acad. Sci. U S A* **106**, 3698–3703 (2009).
- Banoglu, E. & King, R. S. Sulfation of indoxyl by human and rat aryl (phenol) sulfotransferases to form indoxyl sulfate. *Eur. J. Drug Metab. Pharmacokinet.* **27**, 135–140 (2002).
- Niwa, T., Ise, M. & Miyazaki, T. Progression of glomerular sclerosis in experimental uremic rats by administration of indole, a precursor of indoxyl sulfate. *Am. J. Nephrol.* **14**, 207–212 (1994).
- Schroeder, J. C. *et al.* The uremic toxin 3-indoxyl sulfate is a potent endogenous agonist for the human aryl hydrocarbon receptor. *Biochemistry* **49**, 393–400 (2010).
- Lamas, B., Natividad, J. M. & Sokol, H. Aryl hydrocarbon receptor and intestinal immunity. *Mucosal Immunol.* **11**, 1024–1038 (2018).
- Rothhammer, V. *et al.* Type I interferons and microbial metabolites of tryptophan modulate astrocyte activity and central nervous system inflammation via the aryl hydrocarbon receptor. *Nat. Med.* **22**, 586–597 (2016).
- Rothhammer, V. *et al.* Microglial control of astrocytes in response to microbial metabolites. *Nature* **557**, 724 (2018).
- Chyan, Y. J. *et al.* Potent neuroprotective properties against the Alzheimer β -amyloid by an endogenous melatonin-related indole structure, indole-3-propionic acid. *J. Biol. Chem.* **274**, 21937–21942 (1999).
- Bliss, E. S. & Whiteside, E. The gut–brain axis, the human gut microbiota and their integration in the development of obesity. *Front. Physiol.* **9**, 900 (2018).
- Pappolla, M. A. *et al.* Indoles as essential mediators in the gut–brain axis. Their role in Alzheimer's disease. *Neurobiol. Dis.* **156**, 105403 (2021).
- Osadchiy, V., Martin, C. R. & Mayer, E. A. The gut–brain axis and the microbiome: Mechanisms and clinical implications. *Clin. Gastroenterol. Hepatol.* **17**, 322–332 (2019).
- Lin, Y. T. *et al.* Protein-bound uremic toxins are associated with cognitive function among patients undergoing maintenance hemodialysis. *Sci. Rep.* **9**, 20388 (2019).
- Gevi, F., Zolla, L., Gabriele, S. & Persico, A. M. Urinary metabolomics of young Italian autistic children supports abnormal tryptophan and purine metabolism. *Mol. Autism* **7**, 47 (2016).
- Cassani, E. *et al.* Increased urinary indoxyl sulfate (indican): New insights into gut dysbiosis in Parkinson's disease. *Parkinsonism Relat. Disord.* **21**, 389–393 (2015).
- Banoglu, E. & King, R. S. Sulfation of indoxyl by human and rat aryl (phenol) sulfotransferases to form indoxyl sulfate. *Eur. J. Drug Metab. Pharmacokinet.* **27**, 135–140 (2002).
- Adesso, S. *et al.* Indoxyl sulfate affects glial function increasing oxidative stress and neuroinflammation in chronic kidney disease: Interaction between astrocytes and microglia. *Front. Pharmacol.* **8**, 370 (2017).
- Karbowska, M. *et al.* Neurobehavioral effects of uremic toxin–indoxyl sulfate in the rat model. *Sci. Rep.* **10**, 9483 (2020).
- Bobot, M. *et al.* Uremic toxic blood–brain barrier disruption mediated by AhR activation leads to cognitive impairment during experimental renal dysfunction. *J. Am. Soc. Nephrol.* **31**, 1509–1521 (2020).
- Jaglin, M. *et al.* Indole, a signaling molecule produced by the gut microbiota, negatively impacts emotional behaviors in rats. *Front. Neurosci.* **12**, 216 (2018).
- Merchak, A. & Gaultier, A. Microbial metabolites and immune regulation: New targets for major depressive disorder. *Brain Behav. Immunity Health* **9**, 100169 (2020).
- Dunlop, B. W. & Mayberg, H. S. Neuroimaging-based biomarkers for treatment selection in major depressive disorder. *Dialogues Clin. Neurosci.* **16**, 507–518 (2014).
- Bilello, J. A. *et al.* MDDScore: Confirmation of a blood test to aid in the diagnosis of major depressive disorder. *J. Clin. Psychiatry* **76**, e199–206 (2015).

37. Gabbay, V. *et al.* The possible role of the kynurenine pathway in adolescent depression with melancholic features. *J. Child Psychol. Psychiatry Allied Discip.* **51**, 935–943 (2010).
38. Bradley, K. A. L. *et al.* The role of the kynurenine pathway in suicidality in adolescent major depressive disorder. *Psychiatry Res.* **227**, 206–212 (2015).
39. Liu, D. *et al.* Beta-defensin 1, aryl hydrocarbon receptor and plasma kynurenine in major depressive disorder: Metabolomics-informed genomics. *Transl. psychiatry* **8**, 10 (2018).
40. Bhattacharyya, S. *et al.* Metabolomic signature of exposure and response to citalopram/escitalopram in depressed outpatients. *Transl. Psychiatry* **9**, 173 (2019).
41. Dunlop, B. W. *et al.* Predictors of remission in depression to individual and combined treatments (PREdict): Study protocol for a randomized controlled trial. *Trials* **13**, 106 (2012).
42. Dunlop, B. W. *et al.* Effects of patient preferences on outcomes in the Predictors of Remission in Depression to Individual and Combined Treatments (PREdict) study. *Am. J. Psychiatry* **174**, 546–556 (2017).
43. Dunlop, B. W. *et al.* Functional connectivity of the subcallosal cingulate cortex and differential outcomes to treatment with cognitive-behavioral therapy or antidepressant medication for major depressive disorder. *Am. J. Psychiatry* **174**, 533–545 (2017).
44. Hamilton, M. A rating scale for depression. *J Neurol Neurosurg Psychiatry* **23**, 56–62 (1960).
45. Hamilton, M. The assessment of anxiety states by rating. *Br. J. Med. Psychol.* **32**, 50–55 (1959).
46. Maier, W., Buller, R., Philipp, M. & Heuser, I. The Hamilton Anxiety Scale: Reliability, validity and sensitivity to change in anxiety and depressive disorders. *J. Affect. Disord.* **14**, 61–68 (1988).
47. Rush, A. J. *et al.* The inventory for depressive symptomatology (IDS): Preliminary findings. *Psychiatry Res.* **18**, 65–87 (1986).
48. Cox, R. W. AFNI: Software for analysis and visualization of functional magnetic resonance neuroimages. *Comput. Biomed. Res.* **29**, 162–173 (1996).
49. Cox, R. W. & Hyde, J. S. Software tools for analysis and visualization of fMRI data. *NMR Biomed.* **10**, 171–178 (1997).
50. Desikan, R. S. *et al.* An automated labeling system for subdividing the human cerebral cortex on MRI scans into gyral based regions of interest. *Neuroimage* **31**, 968–980 (2006).
51. Taylor, P. A. & Saad, Z. S. FATCAT: (an efficient) functional and tractographic connectivity analysis toolbox. *Brain Connect.* **3**, 523–535 (2013).
52. Fiehn, O. Metabolomics by gas chromatography–mass spectrometry: Combined targeted and untargeted profiling. *Curr. Protoc. Mol. Biol.* **114**, 30–34 (2016).
53. Fiehn, O. *et al.* Quality control for plant metabolomics: Reporting MSI-compliant studies. *Plant J.* **53**, 691–704 (2008).
54. Lai, Z. *et al.* Identifying metabolites by integrating metabolome databases with mass spectrometry cheminformatics. *Nat. Methods* **15**, 53–56 (2018).
55. Fan, S. *et al.* Systematic error removal using random forest for normalizing large-scale untargeted lipidomics data. *Anal. Chem.* **91**, 3590–3596 (2019).
56. MahmoudianDehkordi, S. *et al.* Alterations in acylcarnitines, amines, and lipids inform about mechanism of action of citalopram/escitalopram in major depression. *Transl. Psychiatry* **11**, 153 (2021).
57. Aickin, M. & Gensler, H. Adjusting for multiple testing when reporting research results: The Bonferroni vs Holm methods. *Am. J. Public Health* **86**, 726–728 (1996).
58. Rosseel, Y. Javaan: An R package for structural equation modeling and more. *J. Stat. Softw.* **48**, 1–36 (2012).
59. Mahmoudian Dehkordi, S. *et al.* Altered bile acid profile associates with cognitive impairment in Alzheimer's disease: An emerging role for gut microbiome. *Alzheimers Dement.* **15**, 76–92 (2019).
60. Nho, K. *et al.* Altered bile acid profile in mild cognitive impairment and Alzheimer's disease: Relationship to neuroimaging and CSF biomarkers. *Alzheimers Dement.* **15**, 232–244 (2019).
61. Ascher, S. & Reinhardt, C. The gut microbiota: An emerging risk factor for cardiovascular and cerebrovascular disease. *Eur. J. Immunol.* **48**, 564–575 (2018).
62. Heianza, Y., Ma, W., Manson, J. E., Rexrode, K. M. & Qi, L. Gut microbiota metabolites and risk of major adverse cardiovascular disease events and death: A systematic review and meta-analysis of prospective studies. *J. Am. Heart Assoc.* **29**, e004947 (2017).
63. Wikoff, W. R. *et al.* Metabolomics analysis reveals large effects of gut microflora on mammalian blood metabolites. *Proc. Natl. Acad. Sci. USA* **106**, 3698–3703 (2009).
64. Elsdon, S. R., Hilton, M. G. & Waller, J. M. The end products of the metabolism of aromatic amino acids by clostridia. *Arch. Microbiol.* **107**, 283–288 (1976).
65. Morawetz, C., Bode, S., Derntl, B. & Heekeren, H. R. The effect of strategies, goals and stimulus material on the neural mechanisms of emotion regulation: A meta-analysis of fMRI studies. *Neurosci. Biobehav. Rev.* **72**, 111–128 (2017).
66. Vogt, K. M., Becker, C. J., W. A. D. & Ibinson, J. W. Human posterior insula functional connectivity differs between electrical pain and the resting state. *Brain Connect.* **6**, 786–794 (2016).
67. Strigo, I. A., Simmons, A. N., Matthews, S. C., Arthur, D. & Paulus, M. P. Association of major depressive disorder with altered functional brain response during anticipation and processing of heat pain. *Arch. Gen. Psychiatry* **65**, 1275–1284 (2008).
68. Shirer, W. R., Ryali, S., Rykhlevskaia, E., Menon, V. & Greicius, M. D. Decoding subject-driven cognitive states with whole-brain connectivity patterns. *Cereb. Cortex* **22**, 158–165 (2012).
69. Wager, T. D. *et al.* An fMRI-based neurologic signature of physical pain. *N. Engl. J. Med.* **368**, 1388–1397 (2013).
70. Alvarez, R. P. *et al.* Increased anterior insula activity in anxious individuals is linked to diminished perceived control. *Transl. Psychiatry* **5**, e591 (2015).
71. Arnold Anteraper, S. *et al.* Hyper-connectivity of subcortical resting-state networks in social anxiety disorder. *Brain Connect.* **4**, 81–90 (2014).
72. Cunningham, R., Windischberger, C., Deecke, L. & Moser, E. The preparation and readiness for voluntary movement: A high-field event-related fMRI study of the Bereitschafts-BOLD response. *Neuroimage* **20**, 404–412 (2003).
73. Misra, G. & Coombes, S. A. Neuroimaging evidence of motor control and pain processing in the human midcingulate cortex. *Cereb. Cortex* **25**, 1906–1919 (2015).
74. Dum, R. P., Levinthal, D. J. & Strick, P. L. Motor, cognitive, and affective areas of the cerebral cortex influence the adrenal medulla. *Proc. Natl. Acad. Sci. USA* **113**, 9922–9927 (2016).
75. Pierson, A. *et al.* Loss of control of pre-motor activation in anxious agitated and impulsive depressives. A clinical and ERP study. *Prog. Neuro-Psychopharmacol. Biol. Psychiatry* **18**, 1037–1050 (1994).
76. Hultin, L. *et al.* Neuromagnetic localization of the late component of the contingent negative variation. *Electroencephalogr. Clin. Neurophysiol.* **98**, 425–448 (1996).
77. Ma, Z. *et al.* Identifying generalized anxiety disorder using resting state habenular circuitry. *Brain Imaging Behav.* **14**, 1406–1418 (2020).
78. Muzzarelli, L., Tettamanti, M., Taddei, M. & Battaglia, M. The emotional processing network at the onset of social anxiety disorder: A combined diffusion tensor imaging and functional connectivity study. *Eur. Neuropsychopharmacol.* **26**, S328–S329 (2016).
79. Moseley, R., Carota, F., Hauk, O., Mohr, B. & Pulvermüller, F. A role for the motor system in binding abstract emotional meaning. *Cereb. Cortex* **22**, 1634–1647 (2012).
80. Drabant, E. M. *et al.* Experiential, autonomic, and neural responses during threat anticipation vary as a function of threat intensity and neuroticism. *Neuroimage* **55**, 401–410 (2011).

81. Seeley, W. W. *et al.* Dissociable intrinsic connectivity networks for salience processing and executive control. *J. Neurosci.* **27**, 2349–2356 (2007).
82. Cauda, F. *et al.* Functional connectivity of the insula in the resting brain. *Neuroimage* **55**, 8–23 (2011).
83. Singer, T., Critchley, H. D. & Preusschoff, K. A common role of insula in feelings, empathy and uncertainty. *Trends Cogn. Sci.* **13**, 334–340 (2009).
84. Kurth, F., Zilles, K., Fox, P. T., Laird, A. R. & Eickhoff, S. B. A link between the systems: Functional differentiation and integration within the human insula revealed by meta-analysis. *Brain Struct. Funct.* **214**, 519–534 (2010).
85. Alhadeff, A. L. *et al.* A neural circuit for the suppression of pain by a competing need state. *Cell* **173**, 140–152 (2018).
86. Nguyen, V. T., Breakspear, M. & Cunnington, R. Reciprocal interactions of the SMA and cingulate cortex sustain premovement activity for voluntary actions. *J. Neurosci.* **34**, 16397–16407 (2014).

Acknowledgements

We acknowledge the editorial services of Mr. Jon Kilner, MS, MA (Pittsburgh) and the assistance of Ms. Lisa Howerton (Duke). This work was funded by grant support to Dr. Rima Kaddurah-Daouk (PI) through NIH grants R01MH108348, R01AG046171 and U01AG061359. Dr. Boadie Dunlop has support from NIH grants P50-MH077083 (PI Mayberg), R01-MH080880 (PI Craighead), UL1-RR025008 (PI Stevens), M01-RR0039 (PI Stevens) and the Fuqua Family Foundations. A preprint of this manuscript is available on bioRxiv (<https://doi.org/10.1101/2020.12.08.388942>).

Author contributions

C.R.B. did analysis of data and helped write the manuscript; O.F. and his team generated biochemical data and wrote its methods and helped with interpretation of findings; H.S.M., W.E.C., J.C., K.S.C. and B.W.D. did analysis connecting metabolomics data to imaging data and helped with writing of manuscript; S.M.D., S.B. and H.S. helped with background literature searches and with interpretation of findings; R.R.K., B.W.D. and A.J.R. helped with interpretation of findings and clinical relevance; R.K.D. is P.I. for project helped with concept development, study design, data interpretation and connecting biochemical and clinical data, and with writing of manuscript.

Competing interests

Dr. Dunlop has received research support from Acadia, Compass, Aptinyx, NIMH, Sage, and Takeda, and has served as a consultant to Greenwich Biosciences, Myriad Neuroscience, Otsuka, Sage, and Sophren Therapeutics. Dr. Rush has received consulting fees from Compass Inc., Curbstone Consultant LLC, Emmes Corp., Holmusk, Johnson and Johnson (Janssen), Liva-Nova, Neurocrine Biosciences Inc., Otsuka-US, Sunovion; speaking fees from Liva-Nova, Johnson and Johnson (Janssen); and royalties from Guilford Press and the University of Texas Southwestern Medical Center, Dallas, TX (for the Inventory of Depressive Symptoms and its derivatives). He is also named co-inventor on two patents: U.S. Patent No. 7,795,033: Methods to Predict the Outcome of Treatment with Antidepressant Medication, Inventors: McMahon FJ, Laje G, Manji H, Rush AJ, Paddock S, Wilson AS; and U.S. Patent No. 7,906,283: Methods to Identify Patients at Risk of Developing Adverse Events During Treatment with Antidepressant Medication, Inventors: McMahon FJ, Laje G, Manji H, Rush AJ, Paddock S. Dr. Mayberg receives consulting and intellectual property licensing fees from Abbott Neuromodulation. Dr. Krishnan is a holder of number of patents in the metabolomic and brain computer interface space some of which have been licensed to Chymia LLC and sublicensed to Psyprotalix. Dr. Kaddurah-Daouk is an inventor on a series of patents on use of metabolomics for the diagnosis and treatment of CNS diseases and holds equity in Metabolon Inc. The other authors declare no competing interests.

Additional information

Supplementary Information The online version contains supplementary material available at <https://doi.org/10.1038/s41598-021-99845-1>.

Correspondence and requests for materials should be addressed to B.W.D. or R.K.-D.

Reprints and permissions information is available at www.nature.com/reprints.

Publisher's note Springer Nature remains neutral with regard to jurisdictional claims in published maps and institutional affiliations.



Open Access This article is licensed under a Creative Commons Attribution 4.0 International License, which permits use, sharing, adaptation, distribution and reproduction in any medium or format, as long as you give appropriate credit to the original author(s) and the source, provide a link to the Creative Commons licence, and indicate if changes were made. The images or other third party material in this article are included in the article's Creative Commons licence, unless indicated otherwise in a credit line to the material. If material is not included in the article's Creative Commons licence and your intended use is not permitted by statutory regulation or exceeds the permitted use, you will need to obtain permission directly from the copyright holder. To view a copy of this licence, visit <http://creativecommons.org/licenses/by/4.0/>.

© The Author(s) 2021

the Mood Disorders Precision Medicine Consortium

Brenda Penninx¹⁶, Elizabeth Binder¹⁷, Gabi Kastenmüller¹⁸, Matthias Arnold^{5,18}, Alejo Nevado-Helgado¹⁹, Colette Blach⁵, Yuri Milaneschi¹⁶, Janine Knauer-Arloth¹⁷, Rich Jansen¹⁶, Dennis Mook-Kanamori²⁰, Xianlin Han²¹, Rebecca Baillie²² & Piero Rinaldo²³

¹⁶Department of Psychiatry, Amsterdam UMC, Vrije Universiteit Amsterdam, Amsterdam, The Netherlands.

¹⁷Max Planck Institute of Psychiatry, Munich, Germany. ¹⁸Institute of Computational Biology, Helmholtz Zentrum München, German Research Center for Environmental Health, Neuherberg, Germany. ¹⁹Department of Psychiatry, University of Oxford, Oxford, UK. ²⁰Leiden University Medical Center, Leiden University, Leiden, The Netherlands.

²¹University of Texas Health Science Center at San Antonio, San Antonio, TX, USA. ²²Rosa & Co., LLC, San Carlo, USA. ²³Biochemical Genetics Laboratory, Department of Laboratory Medicine and Pathology, Mayo Clinic, Rochester, MN, USA.